# Arctic Cloud Changes from Surface and Satellite Observations

RYAN EASTMAN AND STEPHEN G. WARREN

*Department of Atmospheric Sciences, University of Washington, Seattle, Washington*

(Manuscript received 1 December 2009, in final form 20 April 2010)

ABSTRACT

Visual cloud reports from land and ocean regions of the Arctic are analyzed for total cloud cover. Trends and interannual variations in surface cloud data are compared to those obtained from Advanced Very High Resolution Radiometer (AVHRR) and Television and Infrared Observation Satellite (TIROS) Operational Vertical Sounder (TOVS) satellite data. Over the Arctic as a whole, trends and interannual variations show little agreement with those from satellite data. The interannual variations from AVHRR are larger in the dark seasons than in the sunlit seasons (6% in winter, 2% in summer); however, in the surface observations, the interannual variations for all seasons are only 1%–2%. A large negative trend for winter found in the AVHRR data is not seen in the surface data. At smaller geographic scales, time series of surface- and satellite-observed cloud cover show some agreement except over sea ice during winter. During the winter months, time series of satellite-observed clouds in numerous grid boxes show variations that are strangely coherent throughout the entire Arctic.

## 1. Introduction

Arctic climate change has been among the most substantial of anywhere on earth in the past two decades. A companion paper, Eastman and Warren (2010, hereafter EW10) has shown that cloud changes derived from surface observations (SURF) appear to be enhancing the warming seen in the Arctic. EW10 show an increasing trend in Arctic total cloud cover and a positive correlation between total cloud cover and surface air temperature in autumn, winter, and spring. Kay and Gettelman (2009) as well as EW10 suggest the presence of a positive cloud response to diminished sea ice extent during autumn. Significant trends in recent decades are observed in both Arctic sea ice and Arctic surface air temperature. Sea ice extent has shown a strong declining trend since the 1980s (Stroeve et al. 2008; NSIDC 2009a,b). Surface air temperature has been observed to increase at a rate of 0.5°C decade$^{-1}$ by the International Arctic Buoy Programme (Rigor et al. 2000) and at a rate of 0.8°C decade$^{-1}$ according to the National Centers for Environmental Prediction–National Center for Atmospheric Research (NCEP–NCAR) reanalysis (Kalnay et al. 1996). Given the relationships between clouds and both sea ice and surface temperature, it is likely that decadal trends in cloud cover are present and are a factor in Arctic climate change.

General circulation models have predicted changes in Arctic climate accompanying rising atmospheric greenhouse gases. Increases in cloud cover and cloud thickness are consistently predicted (Vavrus 2004; Vavrus et al. 2008a,b; Gorodetskaya and Tremblay 2008) in the coming century; these predictions are summarized in greater detail in EW10. Feedbacks are present in the Arctic climate system, which likely create a complex climate response to greenhouse-gas-induced global warming. Climate variations such as ENSO and the North Atlantic Oscillation can impose yearly or decadal-scale fluctuations in Arctic climate and cloud cover. Because of these variations and feedbacks, changes in Arctic climate are not likely to be exactly linear. However, simple measures of changes in cloud cover are needed to compare observations to modeled climate responses. An analysis of linear trends is commonly presented to facilitate such a comparison.

Results from existing studies of decadal trends in total cloud cover indicate that there is likely significant disagreement among data sources. Some studies have analyzed clouds over the entire Arctic, defined as all area north of 60°N, while others have focused on just the oceanic regions of the Arctic. No two existing studies have analyzed the same period. Two studies based on

*Corresponding author address:* Ryan Eastman, Department of Atmospheric Sciences, University of Washington, Box 351640, Seattle, WA 98195-1640.
E-mail: rmeast@atmos.washington.edu

DOI: 10.1175/2010JCLI3544.1

satellite retrievals of total cloud cover—(i) over the oceans between 1980 and 2001 (Schweiger 2004) and (ii) over all of the Arctic between 1982 and 1999 (Wang and Key 2005)—agree in finding a strong decreasing trend in cloud cover during winter as well as a substantial increase in spring cloud cover. Our companion paper EW10, based on surface-observed clouds, has found slight increases for all seasons in total cloud cover both over the Arctic Ocean and over the Arctic as a whole. The only season showing consistent agreement among the three datasets is summer, when a slight positive trend is seen. The magnitudes and signs of the previously published winter and spring trends in total cloud cover disagree substantially. We believe this disagreement requires examination given the possible climatic implications of changing cloud cover.

The warming or cooling effect of changes in cloud cover depends upon the season of the change. Clouds can cool the surface by scattering incoming shortwave radiation. Clouds can warm the surface by absorbing longwave radiation emitted from the surface and reemitting the radiation back downward. Numerous studies have attempted to quantify these effects and to establish the timing and duration of the periods where clouds cool versus warm the Arctic (Curry and Ebert 1992; Intrieri et al. 2002; Schweiger and Key 1994; Vavrus 2004; Walsh and Chapman 1998; Wang and Key 2003; Dong et al. 2010). Though no two studies agree exactly, it is likely that Arctic clouds produce a net cooling during summer when the surface has melted and the sun is high [June–August (JJA)] and a warming throughout the rest of the year when the sun is low or below the horizon. The temperature–cloud cover correlations shown in EW10 substantiate this claim, though summer correlations were not significant because of minimal variation in summer surface air temperature. Because of the seasonal dependence of the cloud–temperature relationship, it is necessary that changes in cloud cover be studied for individual seasons over the Arctic and that observed changes be accurate in all seasons.

Clouds can be detected by satellites or by surface observers at weather stations and on ships. In this study, the satellite datasets analyzed are the Television and Infrared Observation Satellite (TIROS) Operational Vertical Sounder Polar Pathfinder (TOVS Path-P; Francis and Schweiger 2009; Schweiger et al. 2002) and the Extended Advanced Very High Resolution Radiometer (AVHRR) Polar Pathfinder (APP-x; Wang and Key 2005). These datasets were chosen because of their long periods of record (relative to other satellite data) over the Arctic, both beginning in the early 1980s. Surface data come from annual and seasonal averages formed from the Extended Edited Synoptic Cloud Reports Archive (Hahn and Warren 2009), beginning in 1971 over land and 1954 over the ocean. Quantitative agreement between surface- and satellite-observed cloud amounts should not be expected because of the different ways in which clouds are defined. However, measures of deviations from the means such as seasonal cycles, decadal trends, and interannual variation may be usefully compared.

Satellite cloud observations offer the advantage of uniform spatial and temporal coverage as well as a high geographical resolution, but they do have some shortcomings in studies of climatic changes. Cloud detection by satellite is difficult over snow and ice surfaces because the clouds cause little change in planetary albedo and also because they cannot be assumed to be colder than the surface. Satellite data are limited when observing Arctic clouds at night, when the APP-x analysis is unable to use the solar channels (TOVS has no solar channels). Time series of satellite data may contain discontinuities when orbits decay and when instruments are replaced on subsequent satellites. Pixel size is a concern, since clouds often exist on scales smaller than the finest resolution attainable by satellite-borne instruments, causing pixels to be partially filled. Finally, the period of record of satellite cloud data over the Arctic begins in 1980 for TOVS and in 1982 for APP-x, while surface observations began 10–30 years earlier.

Surface observations offer a long period of record at consistent locations (weather stations both on land and on sea ice) as well as the availability of cloud-type information. This study will not focus on cloud types, since the satellite data analyzed do not specify cloud types. Clouds can be detected at night from the surface if the moonlight is adequate (Hahn et al. 1995). Cloud observations from the surface are limited by inadequate geographic coverage and by a policy change in North America resulting in the phasing out of visual cloud observations in recent times. Figure 11 of Schweiger et al. (2002) shows a low bias in surface-observed cloud fraction when compared to cloud fraction observed simultaneously by lidar, during the Surface Heat Budget of the Arctic Ocean (SHEBA) experiment in the Arctic Ocean. This bias is partially explained by a lack of adequate moonlight in some of the observations, and by the lidar's inability to distinguish clear-sky ice particle precipitation ("diamond dust") from clouds. This problem could also exist when comparing surface observations to those from satellites, depending on the sensitivities of the satellite detection. Hahn et al. (1995) and Town et al. (2005) also show a low bias that could exceed 5% in cloud amounts observed from the surface during polar night. This bias may hinder the accurate calculation of the seasonal cycle using surface observations, but it is unlikely to affect studies of trends and interannual variations in

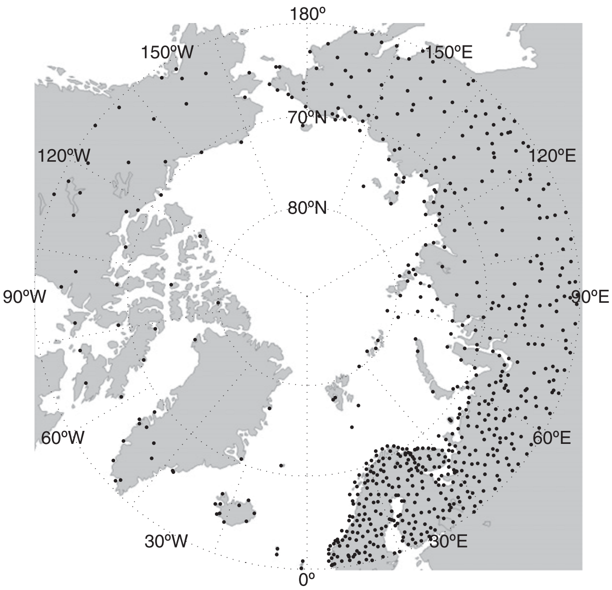


FIG. 1. Distribution of surface stations used throughout the Arctic.

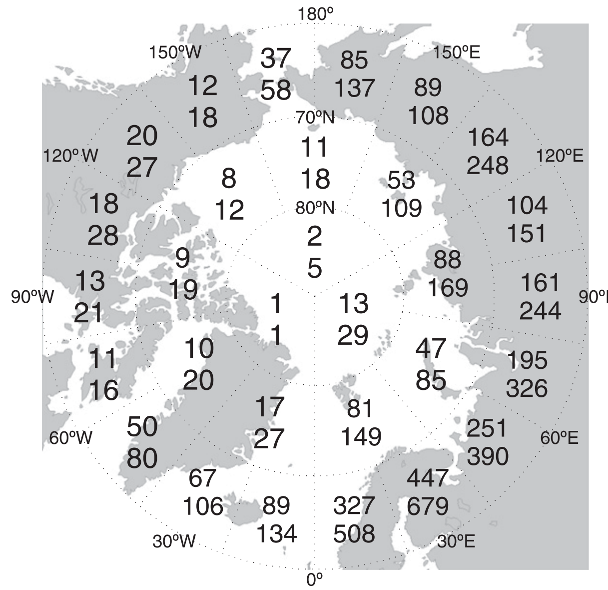


FIG. 2. Average number of observations in hundreds per year during the (top number) dark seasons (SON and DJF) and (bottom number) light seasons (MAM and JJA).

specific seasons, since the bias is consistent from year to year. Surface-observed amounts of low-cloud types, particularly cumulonimbus, have been shown by Bajuk and Leovy (1998) to vary coherently across differing latitude bands on decadal time scales over the ocean. This tendency was not observed in the Arctic cloud analyses in EW10. These large-scale variations are thought to be spurious, but a verifiable explanation has not yet been found. One reason could be the changing fractions of nationalities contributing ship reports over time. Furthermore, reports by individual surface observers may differ even when observing the same clouds, so a meaningful comparison requires a large number of observations to be averaged, which in turn requires averaging over large areas and time spans.

It is the goal of this paper to provide a more comprehensive comparison between surface and satellite datasets, analyzing trends, seasonal cycles, and interannual variations over matching regions for coincident time spans, using data updated as recently as possible.

## 2. Data

Surface-observed cloud data for this study come exclusively from surface synoptic observations reported from weather stations on land, drifting stations on sea ice, and ships. The geographic distribution of weather stations is shown in Fig. 1. The data sources, the methods used to obtain averages and seasonal anomalies, the screening for adequate moonlight in nighttime observations, and the methods used to combine land and ocean data are described in EW10.

Figure 2 shows the average number of cloud observations (in hundreds) per year during the light [March–May (MAM) and JJA] and dark [September–October (SON) and December–February (DJF)] seasons in the Arctic. The sparseness of surface-based cloud observations over remote parts of the Arctic Ocean is evident, especially during the dark season. This geographic variation in numbers of observations highlights a fundamental limitation of surface observations, since it is possible that some remote areas of the Arctic are missed.

From those surface-observed data, we developed a climatology of total cloud cover and the amounts of nine cloud types: five low-cloud types (cumulonimbus, cumulus, stratus, stratocumulus, and fog), three middle types (altocumulus, altostratus, and nimbostratus), and one type for high (cirriform) clouds. For this study, only total cloud cover is compared, since the satellite datasets used do not attempt to identify cloud types.

For a comparison with surface observations, we have chosen two satellite-derived cloud cover time series that have long periods of record over the Arctic. The first satellite dataset is the APP-x data by Wang and Key (2005), spanning the period 1982–2004 on the 25-km Equal-Area Scalable Earth (EASE) grid (Brodzik and Knowles 2002). The AVHRR instrument is carried on polar-orbiting satellites. Two satellite passes per day are used; the daily values were averaged by Wang and Key to form two monthly average cloud-cover values, one for each of the two times. We averaged these two values to form the monthly cloud cover in each grid box. APP-x

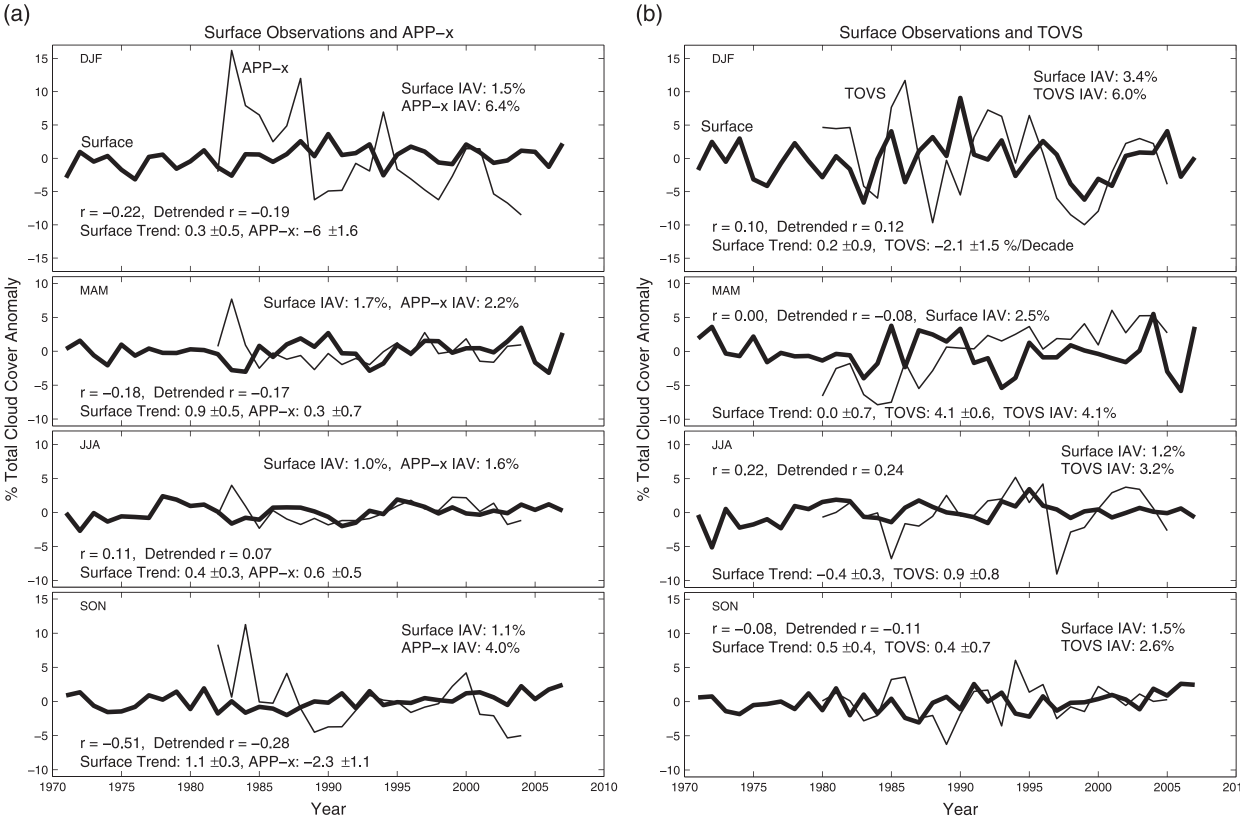


FIG. 3. (a) Anomaly time series of surface-observed Arctic total cloud cover and that observed by APP-x for 60°–90°N. Trends are in percent per decade and calculated only for the overlapping time span (1982–2004). (b) Anomaly time series over Arctic Ocean areas, 60°–90°N, of surface-observed total cloud cover and that observed by the TOVS Path-P. Trends are percent per decade and calculated only for the overlapping time span (1980–2005).

averages covering all land and ocean area north of 60°N were used. Data are available through 2004; the current version was provided by X. Wang and J. R. Key (2009, personal communication).

The second satellite dataset is the TOVS Path-P data spanning 1980–2005 (Francis and Schweiger 2009; Schweiger et al. 2002). TOVS has been used by Schweiger (2004) primarily over ocean areas, though for the purpose of this comparison a grid box on land is also studied. When studying the entire Arctic north of 60°N, we also have elected to use TOVS data just over the ocean because of a lack of TOVS retrievals over higher terrain in North America, including in Alaska and Greenland. TOVS data are organized on the EASE 100-km grid, and for this study, ocean areas are required to be composed of EASE grid boxes made up of 100% ocean cover based on AVHRR global land-cover data on the 1-km EASE grid (Knowles 2004). Daily TOVS cloud cover values are formed based on 24-h average values centered on 1200 UTC for each 100-km EASE grid box. These daily values are then averaged over a month to form monthly total cloud amounts.

## 3. Comparison of surface cloud data with satellite data

We begin with a comparison of yearly anomalies of total cloud cover over the entire Arctic. Yearly anomalies in APP-x data represent all areas north of 60°N, while anomalies for the TOVS data are for ocean areas north of 60°N. Figures 3a and 3b show these anomaly time series plotted along with anomalies of surface-observed total cloud cover over the same regions. The slopes of trend lines (median of pairwise slopes; Lanzante 1996) are given in the figures, fitted for the overlapping period only. Linear correlation coefficients are shown for the detrended time series as well as for the unaltered data to test for any bias associated with instrument- or observer-induced spurious trends.

In Fig. 3a, trends in APP-x data agree in sign and relative magnitude with surface observations during spring and summer. During autumn and winter, by contrast, there is a strong negative trend in the APP-x time series, but a weak positive trend in surface-observed clouds. Interannual variability (IAV; the standard deviation of

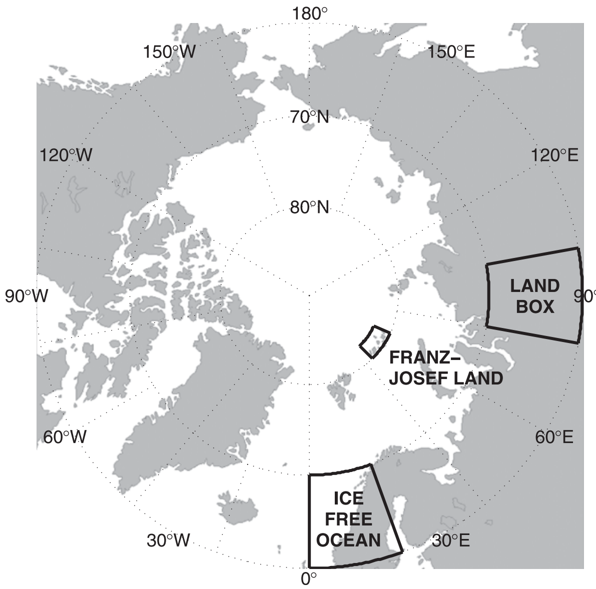


FIG. 4. Regions chosen for comprehensive comparison between surface and satellite cloud data.

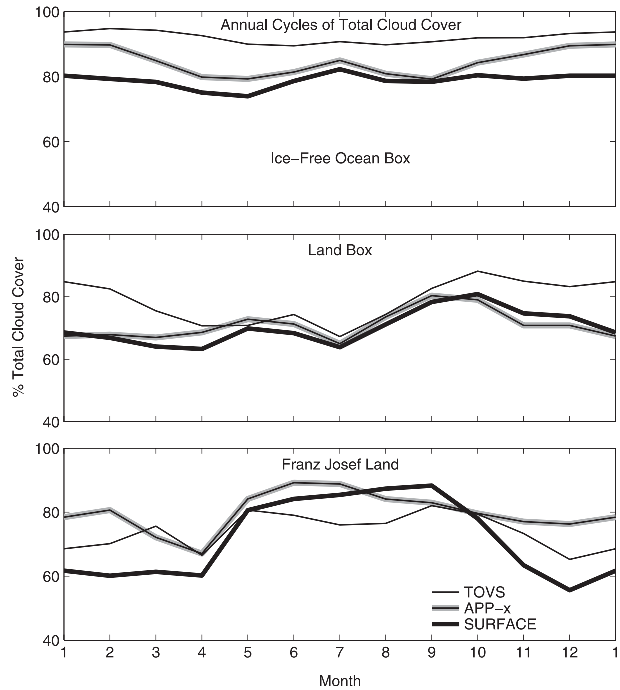


FIG. 5. Annual cycles of total cloud cover over (top) ice-free ocean, (middle) land, and (bottom) ice as detected by TOVS, APP-x, and SURF. The three boxes are defined in Fig. 4.

seasonal means) is also much larger in the APP-x data during autumn and winter. The correlation coefficient ($r$) in summer is very weakly positive. In spring it is weakly negative because of the influence of a few points near the beginning of the APP-x time series. However, when the spring time series are visually compared, some agreement in variation is seen throughout much of the overlapping period. Correlation between surface observations and the APP-x data in winter and autumn is weakly negative.

The trend of total cloud cover over the ocean areas of the Arctic from the TOVS data (Fig. 3b) agrees in sign with that derived from surface observations only in autumn. The springtime trend in TOVS is strongly positive, whereas the surface data show no trend. As was the case in the APP-x data, the IAV for TOVS is much greater in winter. The summer averages from TOVS data show larger IAV than those from APP-x or surface data, mainly due to large negative anomalies in 1985 and 1997, which do not coincide with any strong downward spikes in APP-x data or in the surface observations. During summer the correlations between the TOVS data and surface observations are slightly positive. However, during spring, autumn, and winter, the correlations are essentially zero.

The differences in cloud variations among these datasets may be the result of satellite-based detection errors associated with day versus night cloud detection, inversions of varying strength interfering with remote sensing of temperature profiles, cloud detection over surfaces with variable albedo, or insufficient numbers of surface observations. To investigate these possibilities, we examine three small well-sampled regions with consistent surface characteristics during light and dark seasons. These regions are shown in Fig. 4. The first is a small box including and immediately surrounding the islands of Franz Josef Land, 80°–82°N, 45°–65°E. This region contains three surface stations and has a consistent record from 1971 through 2007, excluding only 2002–04. Franz Josef Land was chosen because of its nearly perpetual ice-bound state, so satellite observations can be compared to one another and surface observations over an icy surface during light and dark seasons. Although the surface of Franz Josef Land is not completely covered with snow and ice year-round, it has been chosen as our ice region because of the large number of observations available from the weather stations on the islands. An oceanic region that is ice free in all seasons (ice-free ocean) was chosen in the Atlantic west of Norway, 60°–70°N, 0°–20°E. Within this box, all satellite and surface observations over land have been excluded so that only measurements over water are compared. During winter the Gulf of Bothnia, which is on the eastern side of this box, is covered in ice, so wintertime observations are excluded past 18°E. Lastly, a land box was chosen (60°–70°N, 80°–100°E). This box was chosen because it had the most observations when compared to other boxes containing 100% land.

Figure 5 shows annual cycles of long-term averaged monthly total cloud cover for each of the three boxes.

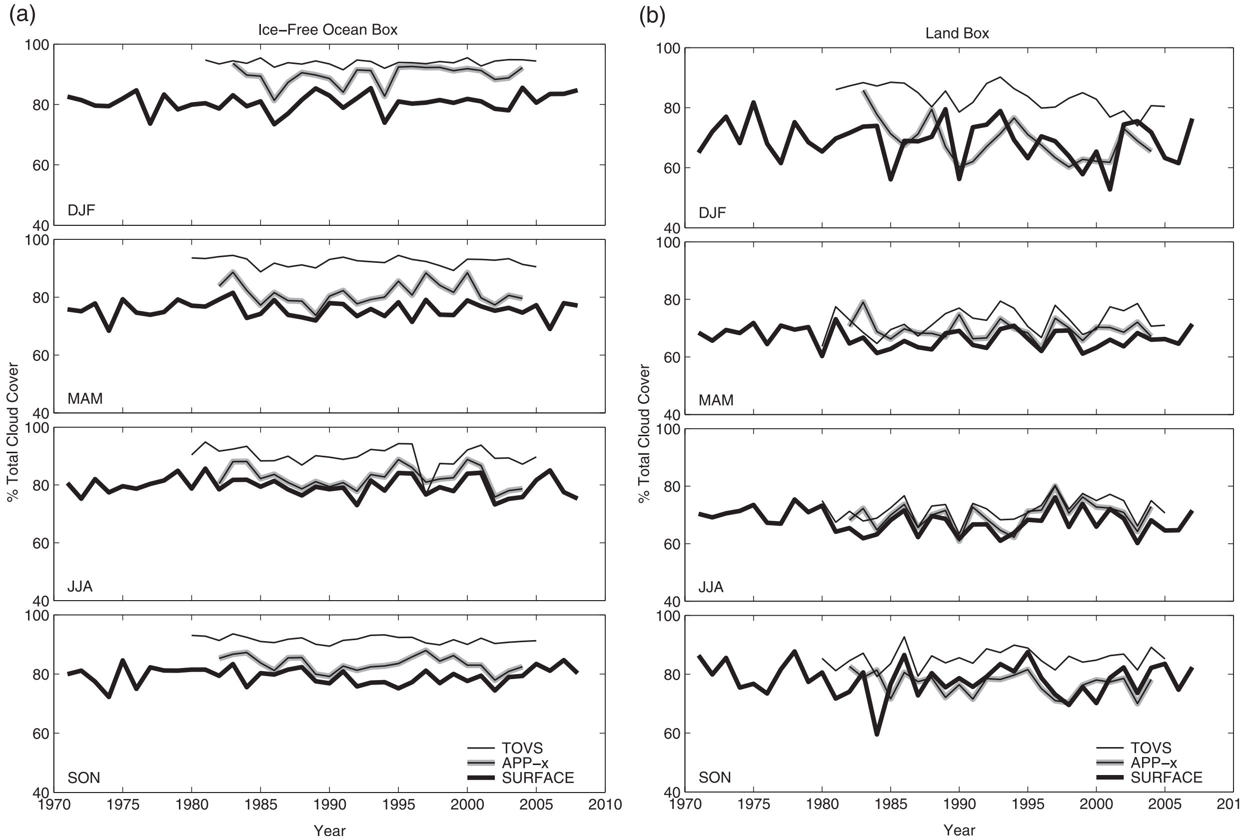


FIG. 6. (a) Time series of total cloud cover during all four seasons as reported by TOVS, APP-x, and SURF over an ice-free ocean surface. (b) As in (a), but over a land surface. (c) As in (a), but over an ice surface.

Over open water, TOVS shows greater cloud cover year-round by 5%–10%, as well as a less prominent annual cycle. The APP-x cycle appears to closely match surface observations during sunlit months, but it resembles TOVS during darker months. In the land box, TOVS is once again showing greater cloud cover, especially during winter months, while the APP-x and surface observations show a nearly identical seasonal cycle. All three datasets agree well between May and September.

Over Franz Josef Land, the yearly cycle displays a distinct ''high Arctic'' pattern (EW10) with a summer maximum in cloud cover and a wintertime minimum. This cycle is prominent in the surface observations, less so with TOVS and APP-x. As was the case over open water, surface observations from Franz Josef Land show less cloud cover during the dark time of the year when compared to satellite data. APP-x shows the greatest cloud cover, especially during winter when APP-x cloud amounts are nearly 10% greater than TOVS, which in turn are nearly 10% greater than the surface observations.

Time series of percent total cloud cover during each season for all three datasets over the three regions are shown in Fig. 6. Seasonal average cloud cover, trends, and correlations for the time series in the figures are all compared in Tables 1–3.

Over the ice-free ocean region (Fig. 6a), higher cloud amounts are diagnosed from the TOVS data throughout the year; surface observations show cloud amounts similar to the APP-x except during winter. As was shown during the annual cycles, surface observations record 5%–10% less cloud cover when compared with satellite observations. Comparing the three boxes, Figs. 6a–c show that the interannual variability over the ocean box is generally lower than over the ice box or the land box. Trends for the period of overlap all agree in sign for the ocean box and also show the lowest magnitude, $<1\%$ decade$^{-1}$ (Table 3c). Correlations among the three time series are positive over the ocean, especially during spring and summer (Table 2c). Surface observations tend to correlate better with the APP-x time series than with TOVS.

Cloud-cover time series for the land box are compared in Fig. 6b. Once again, higher cloud amounts are seen in the TOVS data throughout the year, while APP-x cloud amounts and surface observed amounts more closely

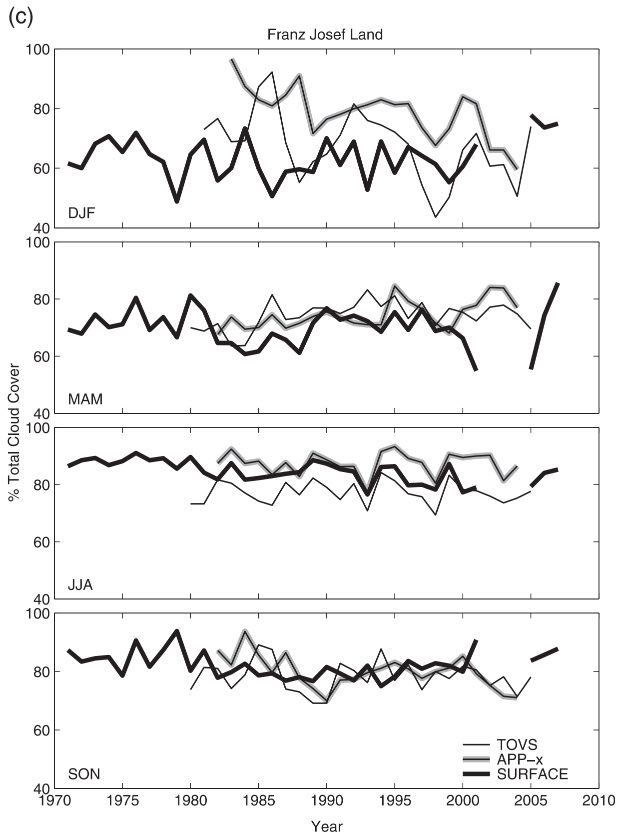


FIG. 6. (*Continued*)

TABLE 1. Comparison of average cloud amounts (%) in three grid boxes for the period 1982–2004 determined from SURF, TOVS (Francis and Schweiger 2009), and APP-x (Wang and Key 2005).

| Franz Josef Land (ice surface) | | | |
|---|---|---|---|
| | SURF | TOVS | APP-x |
| DJF | 62 | 67 | 79 |
| MAM | 68 | 74 | 74 |
| JJA | 83 | 77 | 87 |
| SON | 80 | 78 | 80 |
| Annual | 73 | 74 | 80 |

| Land box (land surface) | | | |
|---|---|---|---|
| | SURF | TOVS | APP-x |
| DJF | 69 | 83 | 69 |
| MAM | 66 | 73 | 69 |
| JJA | 67 | 72 | 70 |
| SON | 77 | 85 | 77 |
| Annual | 70 | 78 | 71 |

| Ocean box (liquid water surface) | | | |
|---|---|---|---|
| | SURF | TOVS | APP-x |
| DJF | 81 | 94 | 90 |
| MAM | 76 | 92 | 81 |
| JJA | 79 | 90 | 82 |
| SON | 79 | 91 | 83 |
| Annual | 79 | 92 | 84 |

agree. Uncertainty of the trends is similar for all three sources throughout the year. The time series all correlate positively with each other, and the correlation coefficients are greater during spring and summer when the Arctic is mostly illuminated by sunlight. TOVS and surface data correlate most strongly except during winter.

Time series of cloud cover detected over the icy surface on and surrounding Franz Josef Land are shown in Fig. 6c. Amounts agree reasonably well between data sources during spring and autumn; however, the APP-x data show a higher cloud amount during winter and the TOVS data show a lower amount during summer. Wintertime trends agree in sign between TOVS and APP-x; however, surface observations show an increase of 1.5% decade$^{-1}$, while the satellites show a large decrease of ~9% decade$^{-1}$. Interannual variability is also larger in all three datasets during wintertime, but more so in the satellite data than in the surface data. All three datasets show clouds increasing during spring for the overlapping period and less substantial trends during summer, with surface observations agreeing with TOVS in summer and disagreeing with both TOVS and APP-x during autumn. The IAV over Franz Josef Land is the highest of all regions; this is at least partly due to the limited areal extent of the defined region. Surface observations and satellite data are positively correlated during spring and summer but uncorrelated during autumn and winter. The correlations between the TOVS and APP-x data are similar to those for the other regions.

The two satellite datasets that were analyzed in this work show a curious pattern, in that all 30 of the 10° Arctic grid boxes show coherent interannual variations during winter (Fig. 7). The time series from surface observations (Fig. 7, third panel) show no such coherence.

## 4. Discussion

Initial comparisons of interannual variations in surface-observed cloud cover with satellite observations over the entire Arctic (60°–90°N) showed poor agreement. The dramatic decreasing trends of total cloud cover observed in winter by both satellite datasets, and which has been previously published, is not seen in the surface data, which shows a slight (nonsignificant) increasing trend over 36 yr (Fig. 3a, top). Also, the strong springtime cloud-cover increase observed in the TOVS dataset is not seen in the surface observations.

The interannual variations in satellite data over the entire Arctic are larger in the dark seasons (autumn and

TABLE 2. Correlation of IAVs of total cloud cover inferred from SURF, APP-x, and TOVS. The value given is the correlation coefficient $r$ multiplied by 100. Time spans are APP-x and SURF, 1982–2004; TOVS and SURF, 1980–2005; and APP-x and TOVS, 1982–2004.

| Franz Josef Land (ice surface) | | | |
|---|---|---|---|
| | APP-x and SURF | TOVS and SURF | TOVS and APP-x |
| DJF | 1 | 0 | 49 |
| MAM | 28 | 41 | 34 |
| JJA | 55 | 46 | 78 |
| SON | 0 | 0 | 44 |
| Mean | 21 | 22 | 51 |

| Land box (land surface) | | | |
|---|---|---|---|
| | APP-x and SURF | TOVS and SURF | TOVS and APP-x |
| DJF | 41 | 23 | 38 |
| MAM | 59 | 78 | 39 |
| JJA | 83 | 91 | 88 |
| SON | 27 | 78 | 41 |
| Mean | 53 | 68 | 52 |

| Ocean box (liquid water surface) | | | |
|---|---|---|---|
| | APP-x and SURF | TOVS and SURF | TOVS and APP-x |
| DJF | 76 | 54 | 65 |
| MAM | 70 | 54 | 52 |
| JJA | 92 | 59 | 52 |
| SON | 48 | 23 | 45 |
| Mean | 72 | 48 | 54 |

TABLE 3. Seasonal average trends (% decade$^{-1}$) from 1982 through 2004 of total cloud cover obtained from SURF, APP-x, and TOVS.

| Franz Josef Land (ice surface) | | | |
|---|---|---|---|
| | SURF | TOVS | APP-x |
| DJF | 1.5 ± 2.3 | −9.4 ± 2.8 | −9.5 ± 2.0 |
| MAM | 3.3 ± 2.2 | 2.9 ± 1.3 | 4.2 ± 1.2 |
| JJA | −1.8 ± 1.3 | −1.0 ± 1.1 | 0.2 ± 1.2 |
| SON | 2.1 ± 1.2 | −1.2 ± 1.6 | −4.3 ± 1.5 |
| Annual | 1.3 ± 1.7 | −2.2 ± 1.7 | −2.3 ± 1.5 |

| Land box (land surface) | | | |
|---|---|---|---|
| | SURF | TOVS | APP-x |
| DJF | −1.4 ± 2.3 | −3.8 ± 0.9 | −4.8 ± 1.9 |
| MAM | 0.8 ± 0.9 | 1.7 ± 1.2 | −0.4 ± 1.1 |
| JJA | 1.4 ± 1.2 | 2.8 ± 1.1 | 1.6 ± 1.4 |
| SON | 0.7 ± 1.9 | 1.0 ± 1.0 | −1.5 ± 1.2 |
| Annual | 0.4 ± 1.6 | 0.4 ± 1.0 | −1.3 ± 1.4 |

| Ocean box (liquid water surface) | | | |
|---|---|---|---|
| | SURF | TOVS | APP-x |
| DJF | 0.2 ± 0.9 | 0.2 ± 0.3 | 1.1 ± 1.1 |
| MAM | −0.1 ± 0.8 | −0.2 ± 0.5 | −0.1 ± 1.2 |
| JJA | −0.5 ± 0.9 | −0.8 ± 1.1 | −0.8 ± 1.2 |
| SON | −0.4 ± 0.7 | −0.6 ± 0.3 | −1.2 ± 0.8 |
| Annual | −0.2 ± 0.8 | −0.3 ± 0.5 | −0.3 ± 1.1 |

winter) than in the sunlit seasons; however, in the surface observations, IAVs for all seasons are similar (Figs. 3a and 3b), despite the large seasonal cycle in the number of surface observations (Fig. 2). Interannual variations in surface-observed cloud anomalies are greater over the ocean when compared to IAVs over the entire Arctic. This is likely because of reduced sampling over the oceanic regions of the Arctic, since reduced spatial and temporal sampling can cause IAVs to appear larger than in reality. In the satellite datasets, year-to-year changes in cloud anomalies over the whole Arctic sometimes exceed 10% in the dark seasons, even though there is no seasonal difference in spatial or temporal sampling. Given the observed increase in IAVs in satellite cloud cover during winter, and the tendency for surface-observed IAVs to remain more constant throughout the year, we conclude that sampling issues are not a likely reason for disagreement between surface and satellite datasets when compared on an Arctic-wide scale.

When the comparison is made in smaller regions, more consistency is seen in IAVs but not in trends. Trends in cloud amounts from the three sources agree over the open-water box but not over the land box, and they are especially conflicting over Franz Josef Land. Correlations between surface and satellite observations also are worst over an icy surface during polar night. The poor agreement over ice during winter could be due to observers at the weather stations not detecting thin clouds in a dark environment, though this was not a problem over other surfaces. In fact, surface observations passing our illuminance criterion over ice should have better light than the equivalent over bare land or ocean since the white surface can reflect incident moonlight, further illuminating a cloud deck. Satellite cloud detection during the polar night can be problematic for the APP-x because of the smaller number of useful channels when sunlight is absent. Infrared cloud detection, such as with TOVS, may also suffer in the presence of strong, shallow temperature inversions, which are common during the polar winter.

The tendency shown in Fig. 7 for satellite cloud amounts in different regions to vary coherently across the Arctic in winter suggests that satellite cloud detection during winter is inadequate for the purposes of finding trends. The geographic coherence of the variations in cloud cover is not observed during sunlit seasons in the satellite data, nor is it ever observed in the Arctic surface data. Similar behavior at much longer time scales has been observed in surface-observed clouds over the oceans by Bajuk and

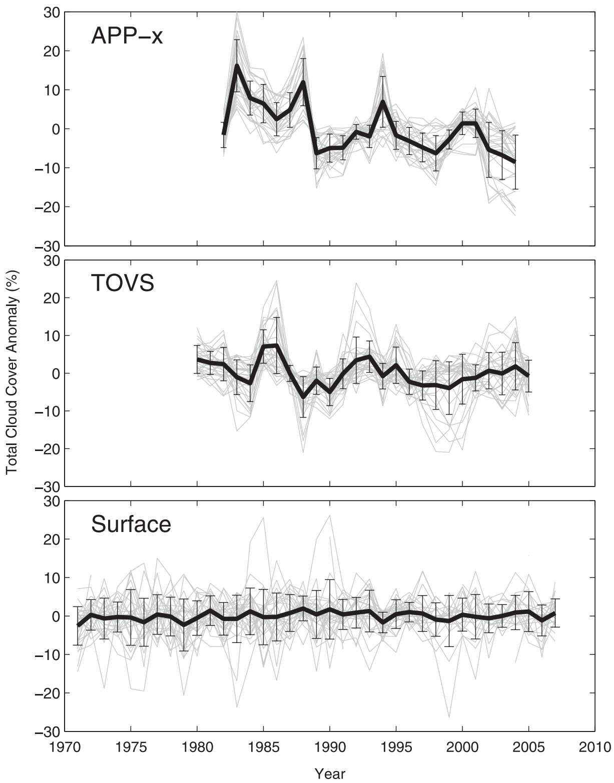


FIG. 7. Surface- and satellite-observed time series of wintertime (DJF) total cloud-cover anomaly for the 30 individual 10° grid boxes shown in Fig. 1 (gray lines), the Arctic average (black line), and the error bars showing the standard deviation of seasonal means.

Leovy (1998), and a testable explanation for such behavior has not been found (Norris 1999). Other data have yet to corroborate the geographically coherent cloud variations seen by Bajuk and Leovy; the trends derived from those data (which mostly follow the long-term coherent variation) are therefore considered spurious. Similarly, we are inclined to attribute the coherent variations seen in the satellite data to nonclimatic causes. In the APP-x data, the largest year-to-year decrease in cloud cover (in 1988–89) coincides with the replacement of a satellite. This indicates the possibility of spurious trends being produced by changes in instrumentation; however, an explanation for the behavior has not yet been put forth by the satellite-cloud-observing community.

The disagreement seen in wintertime cloud-cover trends as observed by surface stations or satellites creates doubt concerning the role of clouds in Arctic climate change during winter. In the Arctic winter, clouds can only affect surface temperature by the downward emission of infrared radiation. This effect is seen in EW10, where Arctic cloud cover correlates positively with surface air temperature in all seasons but summer. The positive correlation remained present when detrended data were used. Trends of surface temperature in the Arctic during winter are positive according to the NCAR reanalysis (Kalnay et al. 1996) as well as the International Arctic Buoy Programme (Rigor et al. 2000). The disagreement in cloud trends seen here casts the role of cloud changes into question as to whether clouds can significantly affect Arctic climate. If clouds are decreasing at the rate seen in the satellite data, then this would indicate that other mechanisms are working to warm the Arctic during winter, and that the role of clouds is much less significant. However, the slight increases seen in the surface data agree physically with the observed temperature trends and would indicate a more significant role for Arctic clouds concerning climate change.

## 5. Conclusions

Interannual variations and trends obtained from satellite observations disagree with those obtained from surface observations when compared for the entire Arctic, especially in the dark seasons (autumn and winter). Better agreement is seen over small geographic regions, except during winter over an icy surface. The exact causes for the disagreement remain unknown; winter/nighttime detection issues or sparse and inadequate surface observations may both be partly responsible. Wintertime cloud cover from satellite data shows a peculiar tendency to vary coherently across the entire Arctic, which may indicate sensor problems during the polar night. We suggest that any user of these data choose a data source based on the desired application. Satellite data may be most useful to detect short-time-scale variations in regions that are poorly sampled from the surface. Further study of all of these datasets is necessary to attempt to improve their accuracies for studies of interannual variations and trends.

*Acknowledgments.* An advance version of the ocean cloud update was provided by Carole Hahn. Axel Schweiger provided TOVS data, and Jeff Key and Xuanji Wang provided updated APP-x data. We thank J. Michael Wallace, Cecilia Bitz, Robert Wood, and Axel Schweiger for their helpful discussion. Xuanji Wang, Jeff Key, Axel Schweiger, and two anonymous reviewers provided helpful comments on the manuscript. The research was supported by NSF's Climate Dynamics Program and NOAA's Climate Change Data and Detection (CCDD) program under NSF Grants ATM-06-30428 and ATM-06-30396.

REFERENCES

Bajuk, L. J., and C. B. Leovy, 1998: Are there real interdecadal variations in marine low clouds? *J. Climate,* **11,** 2910–2921.

Brodzik, M. J., and K. W. Knowles, 2002: EASE-Grid: A versatile set of equal-area projections and grids. *Discrete Global Grids,* M. F. Goodchild and A. J. Kimerling, Eds., National Center for Geographic Information and Analysis.

Curry, J. A., and E. E. Ebert, 1992: Annual cycle of radiation fluxes over the Arctic Ocean: Sensitivity to cloud optical properties. *J. Climate,* **5,** 1267–1280.

Dong, X., B. Xi, K. Crosby, C. N. Long, R. S. Stone, and M. D. Shupe, 2010: A 10-yr climatology of Arctic cloud fraction and radiative forcing at Barrow, Alaska. *J. Geophys. Res.,* in press, doi:10.1029/2009JD013489.

Eastman, R., and S. G. Warren, 2010: Interannual variations of Arctic cloud types in relation to sea ice. *J. Climate,* **23,** 4216–4232.

Francis, J. A., and A. J. Schweiger, cited 2009: TOVS Pathfinder Path-P daily and monthly polar gridded atmospheric parameters. National Snow and Ice Data Center, Boulder, CO. [Available online at http://nsidc.org/data/nsidc-0027.html.]

Gorodetskaya, I. V., and L. B. Tremblay, 2008: Arctic cloud properties and radiative forcing from observations and their role in sea ice decline predicted by the NCAR CCSM3 model during the 21st century. *Arctic Sea Ice Decline: Observations, Projections, Mechanisms, and Implications, Geophys. Monogr.,* Vol. 180, Amer. Geophys. Union, 213–268.

Hahn, C. J., and S. G. Warren, cited 2009: Extended edited synoptic cloud reports from ships and land stations over the globe, 1952-1996. Numerical Data Package NDP-026C, Carbon Dioxide Information Analysis Center (CDIAC). [Available online at http://cdiac.ornl.gov/epubs/ndp/ndp026c/ndp026c.html.]

——, ——, and J. London, 1995: The effect of moonlight on observation of cloud cover at night, and application to cloud climatology. *J. Climate,* **8,** 1429–1446.

Intrieri, J. M., C. W. Fairall, M. D. Shupe, P. O. G. Persson, E. L. Andreas, P. S. Guest, and R. E. Moritz, 2002: An annual cycle of Arctic surface cloud forcing at SHEBA. *J. Geophys. Res.,* **107,** 8039, doi:10.1029/2000JC000439.

Kalnay, E., and Coauthors, 1996: The NCEP/NCAR 40-Year Reanalysis Project. *Bull. Amer. Meteor. Soc.,* **77,** 437–471.

Kay, J. E., and A. Gettelman, 2009: Cloud influence on and response to seasonal Arctic sea ice loss. *J. Geophys. Res.,* **114,** D18204, doi:10.1029/2009JD011773.

Knowles, K., 2004: EASE-Grid land cover data resampled from AVHRR global 1 km land cover, version 2, March 1992 - April 1993. National Snow and Ice Data Center, Boulder CO, digital media. [Available online at http://nsidc.org/data/ease/ease_grid.html.]

Lanzante, J. R., 1996: Resistant, robust and non-parametric techniques for the analysis of climate data: Theory and examples, including applications to historical radiosonde station data. *Int. J. Climatol.,* **16,** 1197–1226.

Norris, J., 1999: On trends and possible artifacts in global ocean cloud cover between 1952 and 1995. *J. Climate,* **12,** 1864–1870.

NSIDC, cited 2009a: Arctic sea ice down to second-lowest extent; likely record-low volume. [Available online at http://nsidc.org/news/press/20081002_seaice_pressrelease.html.]

——, cited 2009b: Arctic sea ice extent. [Available online at http://nsidc.org/images/arcticseaicenews/20090818_Figure2.png.]

Rigor, I., R. Colony, and S. Martin, 2000: Variations in surface air temperature observations in the Arctic, 1979–97. *J. Climate,* **13,** 896–914.

Schweiger, A. J., 2004: Changes in seasonal cloud cover over the Arctic seas from satellite and surface observations. *Geophys. Res. Lett.,* **31,** L12207, doi:10.1029/2004GL020067.

——, and J. Key, 1994: Arctic Ocean radiative fluxes and cloud forcing estimated from the ISCCP C2 cloud dataset, 1983–1990. *J. Appl. Meteor.,* **33,** 948–963.

——, R. W. Lindsay, J. A. Francis, J. Key, J. M. Intrieri, and M. D. Shupe, 2002: Validation of TOVS Path-P data during SHEBA. *J. Geophys. Res.,* **107,** 8041, doi:10.1029/2000JC000453.

Stroeve, J., M. Serreze, S. Drobot, S. Gearheard, M. Holland, J. Maslanik, W. Meier, and T. Scambos, 2008: Arctic sea ice extent plummets in 2007. *Eos, Trans. Amer. Geophys. Union,* **89,** doi:10.1029/2008EO020001.

Town, M. S., V. P. Walden, and S. G. Warren, 2005: Spectral and broadband longwave downwelling radiative fluxes, cloud radiative forcing, and fractional cloud cover over the South Pole. *J. Climate,* **18,** 4235–4252.

Vavrus, S., 2004: The impact of cloud feedbacks on Arctic climate under greenhouse warming. *J. Climate,* **17,** 603–615.

——, M. Holland, and D. Bailey, 2008a: The role of Arctic clouds during intervals of rapid sea ice loss. *Eos, Trans. Amer. Geophys. Union,* **89** (Fall Meeting Suppl.), Abstract C51A0539.

——, D. Waliser, A. Schweiger, and J. Francis, 2008b: Simulations of 20th and 21st century Arctic cloud amount in the global climate models assessed in the IPCC AR4. *Climate Dyn.,* **33,** 1099–1115, doi:10.1007/s00382-008-0475-6.

Walsh, J. E., and W. L. Chapman, 1998: Arctic cloud–radiation–temperature associations in observational data and atmospheric reanalyses. *J. Climate,* **11,** 3030–3045.

Wang, X., and J. R. Key, 2003: Recent trends in Arctic surface, cloud, and radiation properties from space. *Science,* **299,** 1725–1728, doi:10.1126/science.1078065.

——, and ——, 2005: Arctic surface, cloud, and radiation properties based on the AVHRR Polar Pathfinder dataset. Part II: Recent trends. *J. Climate,* **18,** 2575–2593.